2D/3D Image Fusion of X-ray Mammograms with Speed of Sound Images: Evaluation and Visualization

Torsten Hopp[a], Julie Bonn[a], Nicole V. Ruiter[a], Mark Sak[b] and Neb Duric[b]

[a]Karlsruhe Institute of Technology, Institute for Data Processing and Electronics, Karlsruhe, Germany;
[b]Barbara Ann Karmanos Cancer Institute, Department of Radiation Oncology, Detroit, USA

ABSTRACT

Breast cancer is the most common cancer among women. The established screening method to detect breast cancer is X-ray mammography. However, X-ray frequently provides poor contrast of tumors located within glandular tissue. In this case, additional modalities like MRI are used for diagnosis in clinical routine. A new imaging approach is Ultrasound Computer Tomography, generating three-dimensional speed of sound images. High speed of sound values are expected to be an indicator of cancerous structures. Therefore, the combination of speed of sound images and X-ray mammograms may benefit early breast cancer diagnosis. In previous work, we proposed a method based on Finite Elements to automatically register speed of sound images with the according mammograms. The FEM simulation overcomes the challenge that X-ray mammograms show two-dimensional projections of a deformed breast whereas speed of sound images render a three-dimensional undeformed breast in prone position. In this work, 15 datasets from a clinical study were used for further evaluation of the registration quality. The quality of the registration was measured by the displacement of the center of a lesion marked in both modalities. We found a mean displacement of 7.1 mm. For visualization, an overlay technique was developed, which displays speed of sound information directly on the mammogram. Hence, the methodology provides a good basis for multimodal diagnosis using mammograms and speed of sound images. It proposes a guidance tool for radiologists who may benefit from the combined information.

Keywords: Registration, Ultrasound Computer Tomography, Mammography, Image Fusion, Multimodal Diagnosis

1. INTRODUCTION

Breast cancer is the most common cancer among women in Europe and North America.[1] In 2009, approximately 192,000 new cases of invasive breast cancer were diagnosed in the US. Approximately 40,000 women in the US are expected to die from breast cancer every year.[2] Detection of breast cancer in an early state is essential for an effective treatment. The likelihood of metastases is correlated to the size of the tumor.[3] Hence, 5 year relative survival is 95% for tumors smaller than 2 cm, whereas this rate decreases to a relative survival of 66% for tumors greater than 5 cm.[2] The smaller the size of the tumor at the point of diagnosis, the less the likelihood of metastases and the higher the chance of survival.

Today, X-ray mammography is the established screening method for breast cancer diagnosis. However, X-ray frequently provides poor contrast for tumors located within glandular tissue and only provides two-dimensional projection images of a deformed breast. Additionally, Magnetic Resonance Imaging (MRI) is used in clinical routine, offering high contrast of soft tissue and high diagnostic accuracy.[4] In contrast to X-ray mammography, the patient is not exposed to radiation. Yet, MRI is less specific and more expensive than X-ray mammography.[5]

A new approach for breast imaging is Ultrasound Computer Tomography (USCT), which offers three-dimensional volumes of the breast in prone position[6].[7] The imaging is based on numerous ultrasound transducers, which surround the breast within a water bath. The approach of *Duric et al.*[6] uses a ring of transducers, which

torsten.hopp@kit.edu, phone +49 721 608 2 5990, adress: Hermann-von-Helmholtz-Platz 1, Eggenstein-Leopoldshafen 76344, Germany, http://www.ipe.kit.edu/

Medical Imaging 2011: Ultrasonic Imaging, Tomography, and Therapy, edited by Jan D'hooge, Marvin M. Doyley,
Proc. of SPIE Vol. 7968, 79680L · © 2011 SPIE · CCC code: 1605-7422/11/$18 · doi: 10.1117/12.877333

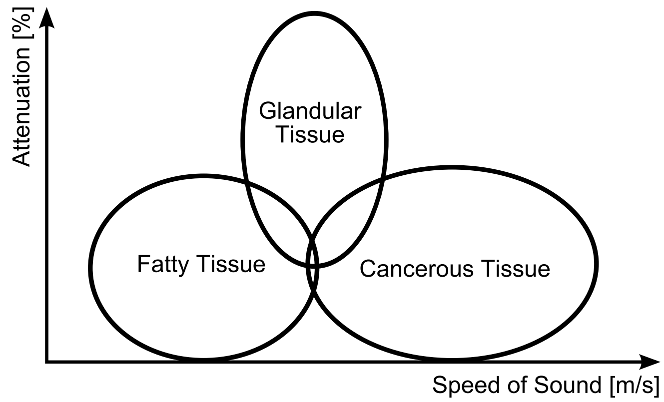

Figure 1: Relation between the ultrasonic properties speed of sound and attenuation for different breast tissues. Adapted and simplified from *Greenleaf et al.*[8]

is translated from the chest wall downwards to acquire multiple slice images. Because of the use of ultrasound, the patient is not subjected to radiation.

USCT provides three types of images: reflection images, attenuation images and speed of sound images. Reflection images reveal changes in the echotexture and are therefore able to image the surface of tissues. This results in the visualization of the morphology. Attenuation and speed of sound images are expected to provide a tissue characterization. As shown in Figure 1, a high speed of sound is expected to be an indicator of cancerous tissue.[8] Additionally, the combination of speed of sound information with attenuation information might further improve the specificity.

The correlation of speed of sound images and X-ray mammograms is challenging due to the different dimensionality and deformation of the breast. Since USCT is still in development, comparison of images with the standard screening method, mammography, is of interest for quality measurement. Furthermore, the combination of diagnostic information may benefit radiological diagnosis. Especially in dense breasts, the speed of sound information may provide guidance for diagnosis of cancerous lesions.

In *Hopp et al.*[9] we presented a method for the registration of X-ray mammograms and speed of sound images based on an algorithm originally designed for the registration of X-ray images and MRI volumes.[10] It is based on a patient-specific biomechanical model of the deformable behavior of the breast to resolve the problem of the huge deformation during mammography. The model is described as Finite Element Model (FEM) and built based on the speed of sound image. It allows the simulation of the deformation of the undeformed breast given in the speed of sound image to achieve a similar configuration as in a corresponding mammogram. A projection of the deformed speed of sound image shows overlaying circumferences with the mammogram so that both modalities can be compared directly. Thus, for example the information about regions of high speed of sound can be used to highlight suspicious regions in the mammogram.

The aim of this work is to evaluate the automatic registration approach with a higher number of datasets and to develop visualization techniques for combined representation of the information in one image to assist radiologists. The central problem in the registration is the large deformation of the breast during mammography. The breast has to be squeezed between two plates and is compressed up to 50% in diameter, which is necessary for a good contrast. This three-dimensional deformation is only recorded as two-dimensional projection. Hence, the individual three-dimensional deformation can not be obtained from these images.

In this paper, section 2 explains the registration approach including the preprocessing, model based registration and visualization. In section 3 we show an evaluation with 15 clinical datasets and first results of the fusion of mammograms with speed of sound images. Finally, section 4 concludes the paper and presents an outlook on current and future work.

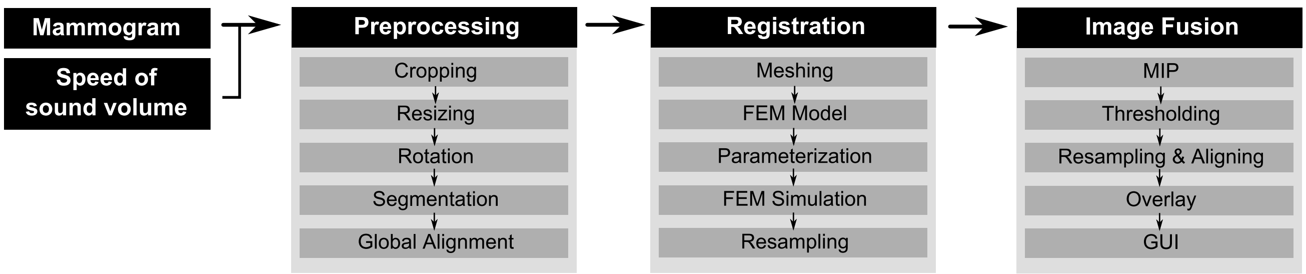

Figure 2: Workflow of the fusion process: first images have to be preprocessed, afterwards the model-based registration is carried out. Finally the visualization process creates the fused images of X-ray mammograms and speed of sound images.

2. METHODS

The challenge of the image registration is that X-ray mammograms show two-dimensional projections of a deformed breast whereas speed of sound images render a three-dimensional undeformed breast. This conflict requires estimating the relation between deformed and undeformed breast applying the deformation to the three-dimensional speed of sound image.

The deformation is determined by a compression simulation using the Finite Element Method (FEM). The underlying patient specific biomechanical model is built on the basis of the preprocessed speed of sound image. The simulation of the deformation is applied to the speed of sound image. Afterwards, the image fusion is carried out (Figure 2).

2.1 Preprocessing

Both, speed of sound image and the X-ray mammogram have to be preprocessed. Images are scaled and rotated to fit the internally used coordinate system. An interpolation is applied to the speed of sound image to overcome the possible gaps between the slices and create isotropic voxels. Afterwards, the images are segmented into background and object. For the mammogram and the speed of sound image, a presegmentation provided by the Karmanos Cancer Institute is used. Based on that, thresholding and morphological operations are applied to smooth the segmentation mask. Partly, corrections of the segmentation had to be carried out by hand.

In a global alignment, the amount of breast tissue shown in the X-ray mammogram and in the three-dimensional speed of sound image is matched. Furthermore, an estimation of the specific projection angle of the X-ray mammogram is carried out.

2.2 Registration

To simulate the compression applied to the breast during mammography, a biomechanical model is built based on the preprocessed speed of sound image. The Finite Element Method is used, since it simulates the physical behavior of the breast.

In order to describe the geometry of the biomechanical model, the three-dimensional speed of sound image is passed to a meshing algorithm. We use a surface oriented meshing to create hexahedral elements. It is based on the transfinite interpolation method,[11] which maps a unit cube to an arbitrary shaped volume. The boundaries of the unit template are mapped to the boundaries of the object. Then uniformly distributed nodes on the unit cube map to nodes on a mesh of the volume, where the curving of the mesh lines is influenced by the curving of the object boundaries.

The physical behavior of a Finite Element model is described by the material model and the boundary conditions. We assume the breast tissue to be an incompressible material that consists mainly of water. Hence, an applied deformation results only in a shape change, not in a change of the volume. The used model approximates the incompressibility with the typical FEM solution using a Poisson's ratio near 0.5. The stress-strain relationship of the breast tissue is described by a neo-hookean material model with material parameters defined by Bakic.[12] Nodes at the back of the model are kept in position to model the fixation of the breast at the chest wall.

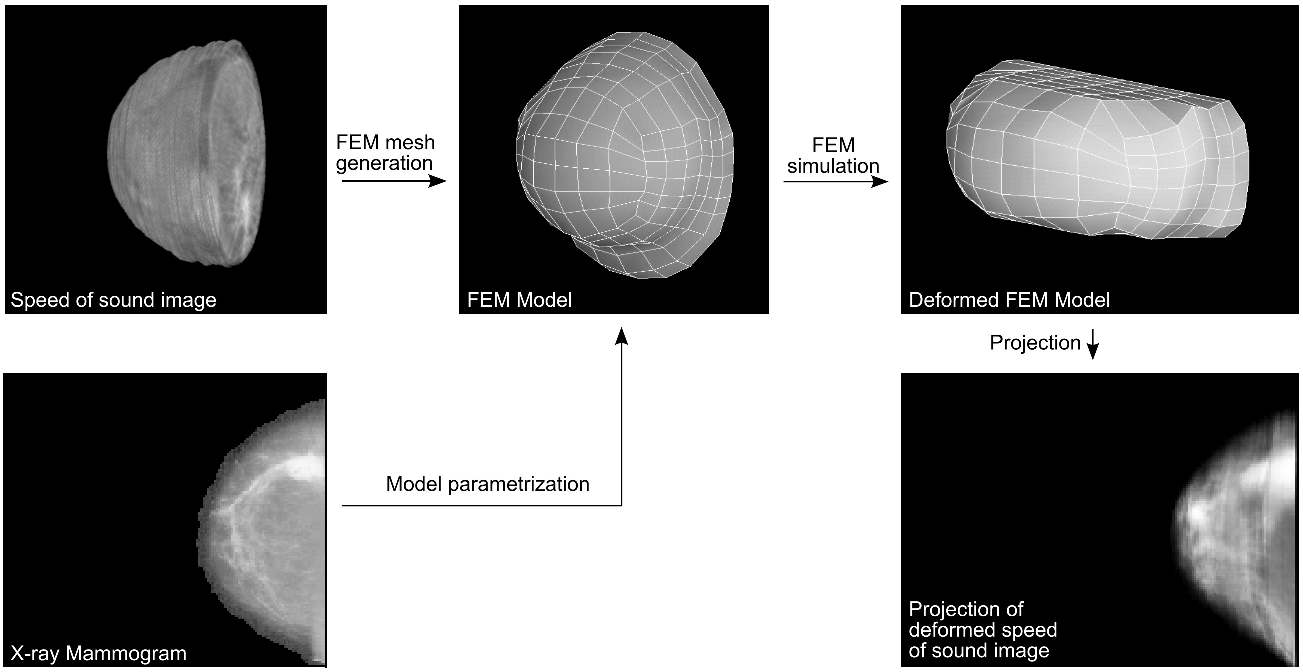

Figure 3: Workflow of the registration process. Based on the speed of sound image (top left), the FEM model is generated by a meshing algorithm. The model (top middle) is parameterized by information from the mammogram (bottom left). A FEM simulation results in a deformed FEM model (top right), which can be used to deform the speed of sound image and create projection images (bottom right) directly comparable to the mammogram.

The mammographic compression is mimicked by a two step approach. In the first step, compression plates are added to the simulation. The deformation is carried out by moving the compression plates until a defined amount of compression is achieved. The thickness of the breast during mammography is readout from the mammogram's meta data if possible. If the information is not present, it has to be estimated. For details refer to *Hopp et al.*[9] In the second step, the shape of the now deformed breast and the circumference of the corresponding mammogram are used to estimate the three-dimensional shape of the breast. The boundary condition is then formulated as displacements between the undeformed and deformed surface of the estimated three-dimensional shape. This results in a projection of the speed of sound image with exactly the same circumference as the segmented mammogram. The workflow describing the registration is illustrated in Figure 3.

The simulation is solved using Ansys.[13] Due to the nonlinear and large deformations, small-step incremental solution methods are used, i.e. the Newton-Raphson method. The resolved deformation field is afterwards applied to calculate the deformed speed of sound image using the transfinite interpolation method.

2.3 Image Fusion

Having finished the image registration, the image fusion starts by creating a maximum intensity projection (MIP) of the deformed speed of sound image (Figure 4). The registration process assures that this projection image overlays congruently with the X-ray mammogram.[9] The resulting projection image contains the highest measured speed of sound values in projection direction. Hence, by resampling the projection image to the size of the mammogram, each pixel in the mammogram can be correlated with a speed of sound value.

As a high speed of sound is expected to be an indicator for cancerous lesions, a threshold is used to extract suspect regions within the projection image. This thresholded image is rendered as a semi-transparent overlay within the mammogram. With a graphical user interface, the particular speed of sound threshold can be chosen manually. This is done, because the usage of a static or automatically chosen patient specific threshold is subject to research.

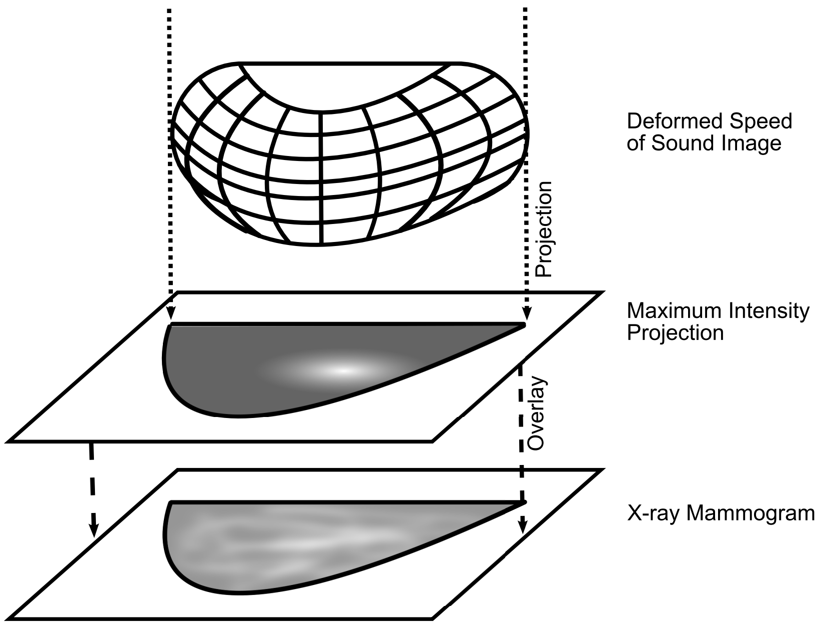

Figure 4: Generation of the speed of sound overlay on mammograms: a projection of the three-dimensional deformed speed of sound image is used to superimpose the original mammogram.

3. RESULTS

For evaluation of the image registration process, 15 datasets from a clinical study[14] of the Karmanos Cancer Institute in Detroit were used. Each dataset includes a speed of sound image and the corresponding cranio-caudal mammogram. Digital as well as analog mammograms were used. The speed of sound images follow the standard acquisition procedure and were presegmented. They have a resolution of 1 mm/pixel at size 221 $\times$ 221 pixel. The number of slices as well as the gap between slices varies depending on the size of the patient's breast. For evaluation purposes, a criterion of inclusion is the visibility of a lesion in both modalities.

The segmentation of the images was generally very challenging. The presegmentation of the speed of sound images had to be partly corrected by hand to obtain the correct and smooth surface of the breast. In the same way, the circumferences of the analog mammograms had to be smoothed. To obtain the final segmented image, morphological operations, de-islanding, and three-dimensional smoothing are applied. The preprocessing is carried out in MATLAB using built-in functionality as well as the iso2mesh toolbox.[15]

The biomechanical models created for the evaluation consist of 216 finite elements, each representing a material model mimicking glandular tissue. Different tissue types within the breast are not considered due to experiments of *Ruiter et al.*[10] stating that there is no major effect in using a more complex model. The described neo-hookean material model using Bakic's[12] material parameters for glandular tissue are applied.

The quality of the registration can be estimated by the accuracy of the registration of lesions visible in both modalities. The provided datasets were reviewed by an expert and the circumference of the lesion was marked. Due to the congruent overlaying of the images after the registration process, the lesion markings can be compared directly. Hence, by measuring the displacement of the centers and the overlap of the lesion marking between the X-ray mammogram and the projection of the deformed speed of sound image, the quality of the registration is estimated. The aim for clinical applicability is a large overlap of the contours and a small deviation between the center position. Resulting images are shown in Figure 5.

3.1 Results of Registration

Using an automated version of the registration software, the mean displacement of the marked centers of lesions is 12.8 mm (SD = 12.0 mm, Median = 9 mm). The mean overlap of the lesion markings is 83%. 12 of 15

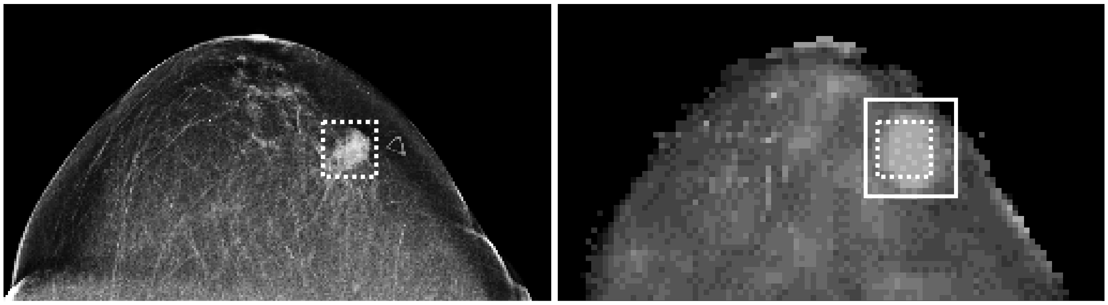

Figure 5: X-ray mammogram (left) with lesion marked by an expert as dotted rectangle. Maximum intensity projection of the deformed speed of sound image (right) with lesion marked by an expert as solid rectangle. As the circumferences of both images overlap congruently, the lesion markings can be compared directly. The overlap, between the marking in the speed of sound image (dotted) and the marking from the mammogram (solid), is 100% in this case.

datasets deliver good registration results with a displacement below 15 mm and an overlap above 85%. For all three outliers, the automatic rotation estimation of the datasets delivers poor results, as only little glandular tissue is visible in theses datasets. As the rotation estimation is based on an image similarity measure, diverse internal structures are essential for an accurate estimation.

By manually correcting the rotation due to patient positioning and uncertain mammographic projection, the mean displacement of the marked centers of lesions could be reduced to 7.1 mm (SD = 5.4 mm, Median = 6 mm). The mean overlap of the lesion markings is 91%. These results validate the previous results presented in *Hopp et al.*[9] and are comparable to the results in *Ruiter et al.*[10]

3.2 Results of Image Fusion

Semitransparent overlay images for the mammograms were created for all 15 datasets. The threshold for the speed of sound was chosen manually to best fit the size of the visible lesion in the mammograms, which is expected to be higher than surrounding glandular and fatty tissue. Resulting images are shown in Figure 6. The thresholded overlays line up well with the mammogram lesions. By visual inspection, the overlap of the thresholded region of high speed of sound and the lesion in the mammography is estimated. For all 15 datasets, the mean overlap is approximately two-thirds. For each dataset a patient specific threshold is used, the mean value to distinguish between the lesion and surrounding tissue is 1520 m/s, the standard deviation is 15.5 m/s and the median is 1515 m/s.

4. CONCLUSION

After promising first results presented in *Hopp et al.*,[9] the now presented evaluation of the image registration of X-ray mammograms with speed of sound images affirms the former results. The average distance between the centers of lesions in the projected speed of sound image and the X-ray mammogram is, for most cases, already acceptable even using automated software. The registration accuracy can be improved using manual corrections of the rotation of datasets to a mean displacement of 7.1 mm and a mean overlap of 91%. Our current research focuses on the improvement of the rotation estimation algorithm to eliminate this manual correction from the workflow.

Against the background of uncertainties from marking the center and size of the lesion in both modalities, we believe these results are already satisfactory.

We furthermore presented an overlay technique to visualize the merged images. Thresholded speed of sound overlay images line up well with marked lesions in the mammograms and cover the lesions at an approximate average of two-thirds. The threshold was chosen specifically for each patient since automatic thresholding is still subject to research. Within a range of 1500 to 1540 m/s, a distinction of suspect tissue to surrounding glandular and fatty tissue was achieved in all cases. We expect the visualization of this quantitative measure to benefit the

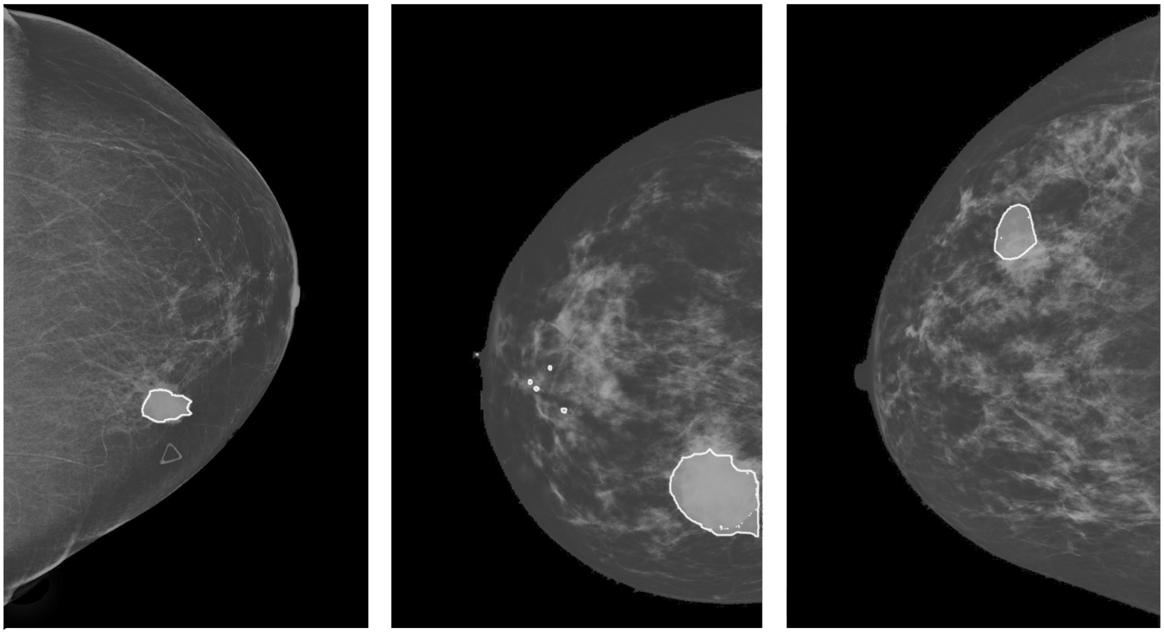

Figure 6: Mammograms of three patients with a semitransparent overlay showing regions with high speed of sound. The thresholded overlay lines up well with the lesions visible in the mammograms.

multimodal diagnosis. The intuitive overlay on a mammogram with its high resolution may guide radiologists in early breast cancer diagnosis.

To the author's knowledge, the evaluation of a method for the registration of three-dimensional speed of sound images and X-ray mammograms has not been done before with a series of 15 datasets from a clinical study. This work validates the applicability of our method to operate well with a variety of datasets and achieve an accuracy which is satisfactory for clinical practice. Furthermore, the information of speed of sound images has never been combined with X-ray mammography in an intuitive and quantitative way. The overlay technique allows a radiologist to explicitly highlight regions of high speed of sound within the mammogram. We expect this information to be beneficial for a more precise multimodal diagnosis, especially for patients with dense breasts. Moreover, using USCT in addition to X-ray mammography may result in a cost reducing, faster and more comfortable examination as USCT does not use contrast agent for a quantitative tissue characterization.

In a next step, the speed of sound overlay has to be investigated for clinical practice by means of a clinical study. In the future, our research will include improvement of the overlay technique to incorporate artifacts in speed of sound images, improvement of the registration algorithm to include oblique mammograms and estimation of lesion positions within the speed of sound image using mammograms from two different projection angles.

ACKNOWLEDGMENTS

This work was partly supported by the German Research Society under grant no. RU 1547/1-1.

REFERENCES

[1] Fischer, T., Bick, U., and Thomas, A., "Mammographie-Screening in Deutschland," *Visions Journal* **15**, 62–67 (2007).

[2] American Cancer Society, "Breast cancer facts and figures 2009 - 2010." Atlanta: American Cancer Society, Inc. (2009).

[3] Sivaramakrishna, R. and Gordon, R., "Detection of breast cancer at a smaller size can reduce the likelihood of metastatic spread: A quantitative analysis"," *Academic Radiology* **4**(1), 8–12 (1997).

[4] DeMartini, W. and Lehman, C., "A review of current evidence-based clinical applications for breast magnetic resonance imaging.," *Top Magn Reson Imaging* **19**, 143–50– (June 2008).

[5] Kaiser, W. A., Fischer, H., Vagner, J., and Selig, M., "Robotic system for biopsy and therapy of breast lesions in a high-field whole-body magnetic resonance tomography unit," *Investigative Radiology* **35**(8), – (2000).

[6] Duric, N., Littrup, P., Poulo, L., Babkin, A., Pevzner, R., Holsapple, E., Rama, O., and Glide, C., "Detection of breast cancer with ultrasound tomography: First results with the computerized ultrasound risk evaluation (C.U.R.E)," *Medical Physics* **34**(2), 773–785 (2007).

[7] Gemmeke, H. and Ruiter, N., "3d ultrasound computer tomography for medical imaging," *Nuclear Instruments and Methods in Physics Research Section A: Accelerators, Spectrometers, Detectors and Associated Equipment* **580**(2), 1057 – 1065 (2007).

[8] Greenleaf, J. F. and Bahn, R. C., "Clinical imaging with transmissive ultrasonic computerized tomography," *Journal of Computer Assisted Tomography* **5**(5), – (1981).

[9] Hopp, T., Holzapfel, M., Ruiter, N. V., Li, C., and Duric, N., "Registration of x-ray mammograms and three-dimensional speed of sound images of the female breast," *Medical Imaging 2010: Ultrasonic Imaging, Tomography, and Therapy* **7629**(1), 762905, SPIE (2010).

[10] Ruiter, N. V., Stotzka, R., Mueller, T. O., Gemmeke, H., Reichenbach, J. R., and Kaiser, W. A., "Model–based registration of x–ray mammograms and mr images of the female breast," *IEEE Transactions on Nuclear Science* **53**, 204 – 211 (2006).

[11] Knupp, P. and Steinberg, S., [*Fundamentals of Grid Generation*], CRC Press, Boca Raton, FL (1994).

[12] Bakic, P. R., *Breast tissue description and modeling in mammography*, PhD thesis, Lehigh University, USA (2000).

[13] Ansys Inc., "Software products." http://www.ansys.com.

[14] Duric, N., Littrup, P., Chandiwala-Mody, P., Li, C., Schmidt, S., Myc, L., Rama, O., Bey-Knight, L., Lupinacci, J., Ranger, B., Szczepanski, A., and West, E., "In-vivo imaging results with ultrasound tomography: report on an ongoing study at the karmanos cancer institute," *Medical Imaging 2010: Ultrasonic Imaging, Tomography, and Therapy* **7629**(1), 76290M, SPIE (2010).

[15] Fang, Q. and Boas, D., "Tetrahedral mesh generation from volumetric binary and grayscale images," *IEEE International Symposium on Biomedical Imaging: From Nano to Macro, 2009. ISBI '09.* , 1142 –1145 (2009).